



The 14th ISAV2024 International Conference on Acoustics and Vibration

11-12 Dec 2024

Karaj - Iran



Topology optimization of piezoelectric materials to improve energy harvesting and actuator effects

Mahmoud Alfouneh¹,

¹ *Mechanical Engineering Department, The University of Zabol, Zabol, Iran*

alfoone@uoz.ac.ir

Abstract

The advances in miniaturization techniques over the last decade have made the widespread of electronic devices which are made based on piezoelectric effect to convert ambient energy (typically vibration) to electric energy as an energy harvester or convert electrical energy to mechanical energy as an actuator. In this regard, topology optimization (TO) is applied to improve piezoelectric devices' energy harvesting and actuating effect. Three TO problems are defined i.e, total displacement minimization of the structure, observation point deflection minimization, and maximizing the electromechanical conversion factor. The objective functions for both the energy harvesting device and actuator are formulated in new formulations in terms of proper physical response functions integrated over the design domain. Such new physical response functions contain electrical and mechanical energies of piezoelectric multilayers comprised of a substrate and a PZT layer. Applying numerical examples shows that it is possible to reach suitable actuation and harvesting devices by deriving the optimal configurations of PZT layers as design domains.

Keywords: PZT, topology optimization, moving iso-surface threshold, actuator energy harvesting.

1. Introduction

Piezoelectric materials have the sophisticated property of converting a form of energy to other forms of energy because of their piezoelectricity phenomenon such as converting vibrational mechanical energy into usable stable electrical energy as energy harvesting devices or applying a voltage to a patch of PZT can lead to a mechanical effect that can be used in many engineering structures. Improving such electromechanical couplings can be obtained by finding the optimal location, size, amount, and shape of the piezoelectric materials that are to be attached as patches to the proposed structure through the TO [1].

TO in the case of designing optimal harvesting devices has been widely investigated in the last decades. Kiyono, et al, studied the design of multilayer piezo composite energy harvesting devices imposing stress constraints [2]. In this study to prevent piezo-ceramic failure due to harmonic vibrations, a global stress constraint was considered. In the study of Noh and Yoon [3], it was found that energy harvesting devices cannot generate DC voltage, and to obtain a continuous voltage, resonant vibrations are required though they cannot be stable sometimes. The problem of charge cancellation due to a combination of tension and compression was investigated by Amlashi, et al [4] by employing TO for a rectangular piezoelectric plate subjected to external in-plan force. Maximizing the electromechanical conversion efficiency as one of the main objective functions in optimization problems of energy harvesting devices was also investigated in the work of Zheng et al [5]. To perform this, both elastic materials alongside piezoelectric materials were considered for the design of energy harvesting devices.

The attempt to maximize the deflection of the whole structure or a chosen point by optimal distribution of PZT material by actuation phenomenon concluded in designing sensors or active vibration control methods. To acquire the best actuation performance by TO of multilayer piezoelectric materials, Kang and Wang [6] considered the material densities and actuation voltages as design variables as well as volume fraction ratio and the control energy as constraints. Luo and Tong used the moving iso-surface threshold method (MIST) [7] to investigate the optimum topological design of morphing piezoelectric structures numerically and experimentally. A novel formulation was presented as the response function in terms of mutual strain energy densities.

In the present investigation, the MIST TO method is applied as the main methodology of the optimization process for two optimization problems, i.e., actuation, and energy harvesting devices. In this regard, three objective functions in terms of physical response function integrated over the design domain are defined which are total structural displacement minimization, observation point deflection minimization, and maximizing the electromechanical coupling efficiency in which the later one is used in energy harvesting devices. Proposed novel formulations of response functions are derived on the basis of strain energies for the total displacement and electromechanical energy conversion maximization and, mutual strain energy densities for the chosen point deflection minimization and are then used to find optimal topologies of piezoelectric materials PZT multilayer structures compromise of a host layer and a PZT layer. For each optimization problem, the related artificial material scenario with penalized mechanical and piezoelectric properties is employed in the topology optimization. Numerical results computed by using MIST are presented for morphing bending and vibrational multilayer plates subjected to mechanical and/or electrical loadings to validate derived formulations and methods for each optimization problem.

2. Analysis and design formulations

2.1 Governing equations

In piezoelectric materials, electrical and mechanical fields are always coupled together. To formulate easily and make simple the computation, it is assumed that the changes in PZT fields and mechanical domain are linear besides, the thermal effects are neglected. By these assumptions, the electro/mechanical field equations are written as:

$$\nabla \cdot \mathbf{T} = \rho \ddot{\mathbf{u}} \quad \text{and} \quad \nabla \cdot \mathbf{D} = 0 \quad (1)$$

In equations (1), \mathbf{T} is the stress tensor, \mathbf{u} is the global displacement vector, ρ is the mass density, and \mathbf{D} is the electrical displacement vector. The above equations also can be written in the form of constitutive PZT law as follows [8]:

$$\mathbf{T} = \mathbf{c}^E \mathbf{S} - \mathbf{e} \mathbf{E} \quad \text{and} \quad \mathbf{D} = \mathbf{e}^T \mathbf{S} + \boldsymbol{\epsilon}^S \mathbf{E} \quad (2)$$

where \mathbf{c}^E is the linear stiffness matrix, \mathbf{e} is the piezoelectric matrix, $\boldsymbol{\epsilon}^S$ is the permittivity matrix, \mathbf{S} is the vector of mechanical strain, \mathbf{E} is the vector of electrical field and \mathbf{T} in equation (2) stands for the matrix transpose in finite element (FE) formulations. In the FE procedure with discretized domain, $\bar{\mathbf{u}} = \mathbf{u} e^{i\omega\tau}$ considered as the displacement, $\bar{\boldsymbol{\phi}} = \boldsymbol{\phi} e^{i\omega\tau}$ as the potential vector variables, and τ denotes time. By utilizing the Lagrange equation of motion and considering the time-harmonic response because of the time-harmonic excitations $\bar{\mathbf{F}} = \mathbf{F} e^{i\omega\tau}$, $\bar{\mathbf{Q}} = \mathbf{Q} e^{i\omega\tau}$, the coupled governing equation of motion in the frequency domain between \mathbf{u} and $\boldsymbol{\phi}$ can be formulated as follows [5]:

$$\left\{ -\omega^2 \begin{bmatrix} \mathbf{M} & 0 \\ 0 & 0 \end{bmatrix} + i\omega \mathbf{C} + \begin{bmatrix} \mathbf{K}_{uu} & \mathbf{K}_{u\phi} \\ \mathbf{K}_{\phi u} & -\mathbf{K}_{\phi\phi} \end{bmatrix} \right\} \begin{bmatrix} \mathbf{u} \\ \boldsymbol{\phi} \end{bmatrix} = \begin{bmatrix} \mathbf{F} \\ \mathbf{Q} \end{bmatrix} \quad \text{or} \quad -\omega^2 \mathbf{M} + i\omega \mathbf{C} + \mathbf{K} \mathbf{u}(\mathbf{u}, \boldsymbol{\phi}) = \mathbf{F} \quad (3)$$

$$\mathbf{M} = \sum_{e=1}^{nel} (\mathbf{m}^e)^{str} + \sum_{e=1}^{nel} (\mathbf{m}^e)^{PZT}, \quad (\mathbf{m}^e)^{str} = \int_{\Omega^e} \rho^{str} \mathbf{H}_u^T \mathbf{H}_u d\Omega, \quad (\mathbf{m}^e)^{PZT} = \int_{\Omega^e} \rho^{PZT} \mathbf{H}_u^T \mathbf{H}_u d\Omega \quad (4)$$

$$\mathbf{K}_{uu} = \sum_{e=1}^{nel} (\mathbf{k}_{uu}^e)^{str} + \sum_{e=1}^{nel} (\mathbf{k}_{uu}^e)^{PZT}, \quad (\mathbf{k}_{uu}^e)^{PZT} = \int_{\Omega^e} \mathbf{B}_u^T \mathbf{c}^E \mathbf{B}_u d\Omega, \quad (\mathbf{k}_{uu}^e)^{STR} = \int_{\Omega^e} \mathbf{B}_u^T \mathbf{D} \mathbf{B}_u d\Omega,$$

$$\mathbf{K}_{u\varphi} = \sum_{e=1}^{nel} \mathbf{k}_{u\varphi}^e, \quad \mathbf{k}_{u\varphi}^e = \int_{\Omega^e} \mathbf{B}_u^T \mathbf{e} \mathbf{B}_\varphi d\Omega, \quad \mathbf{k}_{\varphi u}^e = \int_{\Omega^e} \mathbf{B}_\varphi^T \mathbf{e}^T \mathbf{B}_u d\Omega, \quad \mathbf{K}_{\varphi\varphi} = \sum_{e=1}^{nel} \mathbf{k}_{\varphi\varphi}^e = \int_{\Omega^e} \mathbf{B}_\varphi^T \boldsymbol{\varepsilon}^S \mathbf{B}_\varphi d\Omega$$

where \mathbf{M} , \mathbf{C} , \mathbf{D} , \mathbf{F} , and \mathbf{Q} are global mass, damping, property matrix for host structure, mechanical load, and electrical charges in addition of \mathbf{K}_{uu} , $\mathbf{K}_{u\varphi}$ and $\mathbf{K}_{\varphi\varphi}$ as the structural stiffness matrix including host and PZT, piezoelectric matrix, and electric matrix, respectively where their elemental matrices are denoted by superscript e . \mathbf{B}_u and \mathbf{B}_φ describe the strain-displacement and the electric field-potential transformation matrices. nel is the number of elements in discretized domain, \mathbf{H}_u and ω are mass shape function and angular velocity, respectively. It is obvious that in the static solution, the terms including ω are omitted.

3. Topology optimization

TO is meant to optimally distribute a given amount of PZT or elastic material in the host layer in a system of single or multilayer plate to address the objective function in actuation and energy harvesting optimization problems. TO problems are defined for actuation and harvesting energy devices as follows:

3.1 Actuation

3.1.1 Problem statement

In this optimization problem the aim is to maximize (or minimize in case of the negative sign) the overall output deflection or the output of a selected point in the desired direction by optimally design of PZT or the host layer. As the solution is a static solution therefore $\omega=0$. The integrated design optimization problem can be formulated as: Find $\mathbf{x} = \{x_1, x_2, x_3, \dots, x_e, \dots, x_{nel}\}$ so that

Maximize f subject to:

$$\begin{cases} \mathbf{K} \mathbf{u}(u, \varphi) = \mathbf{F} \\ p_\xi \sum_{e=1}^{nel} x_{e\xi} v_e \leq V_{f\xi} V, \quad \sum_{e=1}^{nel} \left(\sum_{\xi=1}^n x_{e\xi} p_\xi \right) v_e \leq V_f V_0, \quad \hat{\varepsilon} \leq x_{e\xi} \leq 1, \quad (e = 1, 2, \dots, nel), \quad (\xi = 1, 2, \dots, n) \end{cases} \quad (5)$$

In this equation, x_e denotes the weighting coefficient or density of e^{th} ($e=1, 2, 3, \dots, nel$) element in ξ^{th} ($\xi=1, 2, 3, \dots, n$) material or phase with vector \mathbf{x} as the design variables. n is the ultimate number of phases in the design domain while p stands for the percentage of ξ^{th} phase in the design domain which in the case of multi-material, it is equal to one for each material or phase. v_e denotes the area or volume of the e^{th} element; V_f illustrates the volume or area of the given design domain where V_0 is the volume or area of the whole design domain. To refrain the singularity of the stiffness matrix $\hat{\varepsilon} = 1e - 3$. Individual solutions for the actuation optimization problem can be given as follows:

3.1.1.1 First solution

In the first solution for maximizing the overall deflection of the PZT structure, minimizing the overall mechanical strain energy of the PZT layer would be a resolution. The mechanical strain energy of the PZT layer can be written as follows:

$$\Pi^S = \frac{1}{2} \mathbf{u}^T \mathbf{K}_{uu} \mathbf{u} \quad \text{or by using equation (6),} \quad \Pi^S = \frac{1}{2} \sum_{e=1}^{nel} \int_{\Omega^e} (\mathbf{u}^e)^T \mathbf{B}_u^T \mathbf{c}^E \mathbf{B}_u \mathbf{u}^e d\Omega \quad (6)$$

Ω^e is the domain of e^{th} element. The displacement \mathbf{u}^e can be derived from solving equation (5). For each element, we can express the total strain energy Π_e^S as follows:

$$\Pi_e^S = \frac{1}{2} \int_{\Omega^e} (u^e)^T \mathbf{B}_u^T \mathbf{c}^E \mathbf{B}_u u^e d\Omega \quad (7)$$

Substituting equation (7) into equation (6) and assuming that a regular mesh is used and the volume of all elements are the same, we have:

$$\Pi^S = \sum_{e=1}^{nel} (\Pi_e^S) v^e \quad \text{or} \quad \Pi^S = \sum_{e=1}^{nel} \int_{\Omega_e} \Pi_e^S d\Omega \quad (8)$$

The integrand function, Π_e^S in equation (8) is a piecewise constant over each element, and is the value of the integrand function at the element centre, which can be extrapolated over a moving patch of several elements to nodal ones[7]. Hence these nodal values can subsequently be used to construct smooth energy density functions within each element or piecewise smooth functions over the entire domain $\bar{\Pi}^S$. Hence equation (8) can be approximated as:

$$\Pi^S = \int_{\Omega} \bar{\Pi}^S d\Omega \quad (9)$$

and $\bar{\Pi}^S$ is the strain energy density function over the entire design domain.

3.1.1.2 Second solution

f as the objective function for a special point displacement maximization (or minimization in negative sign) at desired direction can be calculated by mutual strain energy density. For a special point i , the displacement at the desired direction can be calculated as follows [7]:

$$u_i = \int_{\Omega} \sigma_i \bar{\epsilon}_i d\Omega = \int_{\Omega} \sigma_r \bar{\epsilon}_i d\Omega \quad (10)$$

where $\sigma_r, \bar{\epsilon}_i$ are the stress and strain fields derived by applying real loading and $\sigma_i, \bar{\epsilon}_i$ are the stress and strain fields produced by applying unit dummy load in point i in the desired direction. For the system (structure) of np points (nodes) u_i as the objective function can be ideally written as follow to meet the proposed objective function mentioned in equation (5):

$$u_i = \int_{\Omega} \left(\sum_{i=1}^{np} \bar{w}_i (\sigma_r \bar{\epsilon}_i)_i \right) d\Omega = \int_{\Omega} \left(\sum_{i=1}^{np} \bar{w}_i (\sigma_i \bar{\epsilon}_i)_i \right) d\Omega \quad \text{where } \bar{w}_i = 1 \text{ is a user-defined coefficient.} \quad (11)$$

3.2 Energy harvesting

3.2.1 Problem formulation

In the energy harvesting optimization problem, to assess the varieties of PZT energy harvesting devices, the energy conversion factor is employed as follows[4]:

$$\eta = \frac{\Pi^E}{W^F} \quad \text{where, } \Pi^E = \frac{1}{2} \phi^T \mathbf{K}_{\phi\phi} \phi, \quad W^F = \Pi^S + \Pi^E \quad \text{and} \quad \Pi^S = \frac{1}{2} u^T \mathbf{K}_{uu} u \quad (12)$$

Here, Π^E is electrical energy, W^F denotes the work performed by an external load and Π^S expresses stored strain energy. Equation (12) also can be written as follows:

$$\eta = \frac{\Pi^E}{\Pi^E + \Pi^S} \quad \text{or} \quad \xi_1 = \frac{1}{\eta} = 1 + \frac{\Pi^S}{\Pi^E} \quad (13)$$

By these definitions, the optimization problem to harvest more electrical energy from the PZT harvesting device can be given as follows:

Find $\mathbf{x} = \{x_1, x_2, x_3, \dots, x_e, \dots, x_{nel}\}$ so that Minimize ξ_1 or maximize $\xi_2 = \frac{\Pi^E}{\Pi^S}$ subject to:

$$\begin{cases} -\omega^2 \mathbf{M} + i\omega \mathbf{C} + \mathbf{K} \bar{\mathbf{u}}(u, \phi) = \bar{\mathbf{F}} \\ p_{\xi} \sum_{e=1}^{nel} x_{e\xi} v_e \leq V_f V, \quad \sum_{e=1}^{nel} \left(\sum_{\xi=1}^n x_{e\xi} p_{\xi} \right) v_e \leq V_f V_0, \quad \hat{\epsilon} \leq x_{e\xi} \leq 1 \end{cases} \quad (14)$$

Referring to the first term of equation (14), minimizing ξ_1 or maximizing ξ_2 can be achieved by minimizing Π^S .

3.3 Method of optimization

The optimization routine used in this study is the MIST algorithm [7], which is an enhanced optimization method that updates the design variables iteratively. One key part of the MIST procedure is to define the physical response function Φ which is the integrand of the objective function over the design domain. In this study as it is obvious, the physical response function for actuation optimization problems and the first resolution is:

$$\Phi_1 = \bar{\Pi}^S \text{ and for the second resolution; } \Phi_2 = \sum_{i=1}^{np} \bar{w}_i (\boldsymbol{\sigma}_r \bar{\boldsymbol{\epsilon}}_i)_i = \sum_{i=1}^{np} \bar{w}_i (\boldsymbol{\sigma}_i \bar{\boldsymbol{\epsilon}}_r)_i \quad (15)$$

Such a physical response function for the energy harvesting device is given as follows:

$$\Phi_3 = \Phi_1 = \bar{\Pi}^S \quad (16)$$

Now, while the physical response functions were established for both optimization problems, optimization problems can be reformulated as a standard MIST method as follows:

Find $\{\mathbf{x}\}$, by using Φ and the iso-surface multi-thresholds $t_\xi < t_{\xi+1}$ ($\xi = 1, 2, 3, \dots, n$), so that

$$\text{Minimize or maximize } f = \int_{\Omega} \Phi S(\Phi, t_1, t_2, t_3, \dots, t_\xi) d\Omega, \quad (17a)$$

$$\text{s. t. } \begin{cases} \mathbf{K} \bar{\mathbf{u}}(u, \varphi) = \bar{\mathbf{F}} & \text{for static solution} \\ -\omega^2 \mathbf{M} + i\omega \mathbf{C} + \mathbf{K} \bar{\mathbf{u}}(u, \varphi) = \bar{\mathbf{F}} & \text{for dynamic solution} \end{cases} \quad (17b)$$

$$p_\xi \sum_{e=1}^{nel} x_{e\xi} v_e \leq V_{f\xi} V, \quad \sum_{e=1}^{nel} \left(\sum_{\xi=1}^n x_{e\xi} p_\xi \right) v_e \leq V_f V_0, \quad \hat{\boldsymbol{\epsilon}} \leq x_{e\xi} \leq 1$$

$S(\Phi, t_1, t_2, t_3, \dots, t_\xi)$ is a step function defined in [7].

3.4 Material model

The material model is based on the well-known SIMP model in which the penalization scheme would differ based on the designed layer. Before presenting the different scenarios based on which layers are under design layers, the structural stiffness matrix, piezoelectric matrix, mass matrix, and electric matrix can be written as follow based on their relevant penalty factor:

$$\mathbf{M} = \sum_{e=1}^{nel} x_e^p (\mathbf{m}^e)^{str} + \sum_{e=1}^{nel} x_e^q (\mathbf{m}^e)^{PZT}, \quad \mathbf{K}_{uu} = \sum_{e=1}^{nel} x_e^r (\mathbf{k}_{uu}^e)^{str} + \sum_{e=1}^{nel} x_e^s (\mathbf{k}_{uu}^e)^{PZT}, \quad \mathbf{K}_{u\varphi} = \sum_{e=1}^{nel} x_e^t \mathbf{k}_{u\varphi}^e, \quad (18)$$

$$\mathbf{K}_{\varphi\varphi} = \sum_{e=1}^{nel} x_e^w \mathbf{k}_{\varphi\varphi}^e$$

Scenario 1: only PZT layer under design layer and static solution, so: $r=0, s=3, t=6$ and $w=4$.

Scenario 2: only PZT layer under design layer and dynamic solution, so: $r=0, s=t=w=3$.

4. Numerical examples and discussion

Numerical examples in this section are provided to validate the derived formulations and methods in actuation and energy harvesting resolutions. The proposed structure is a multilayer plate (depending on the problem can be a single plate) clamped at the left side and it is subjected to actuation voltage and mechanical loads (depending on the example) as seen in Figure 1a.

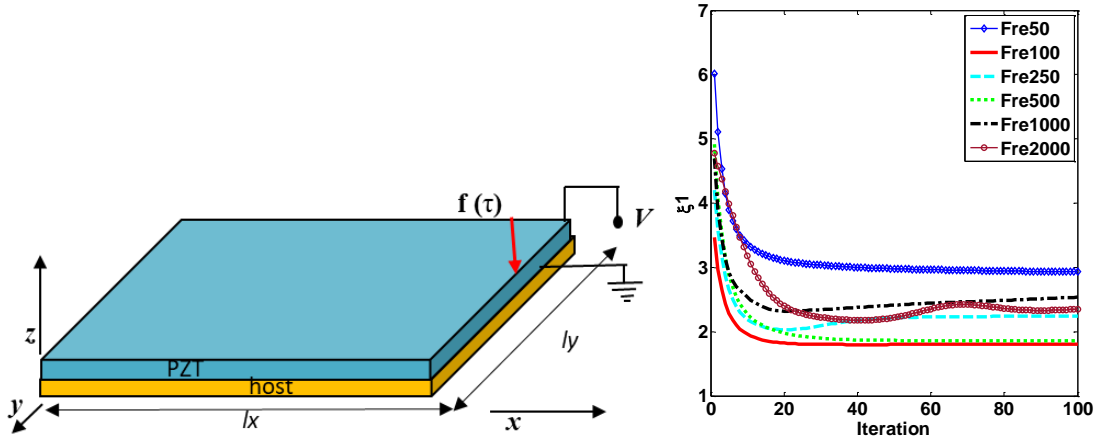


Figure 1a. A substrate plate with PZT sheet. **Figure 1b.** The curves of iteration histories of objective function

In the case of a multilayer plate, one layer is the substrate plate. The geometrical dimensions of the plate are: $l_x=0.4\text{m}$, $l_y=0.3\text{m}$, substrate thickness $=0.0025\text{m}$, and the PZT thickness is 0.0015m . Both the host and PZT layers are discretized by 80×60 elements but with SOLSH190 and SOLID5 ANSYS elements, respectively. The volume constraint is set to 50% of the PZT layer. The elastic, piezoelectric, and dielectric coefficient matrices for the PZT-4 layer are set as follows:

$$c = \begin{bmatrix} 13.2 & 7.1 & 7.3 & 0 & 0 & 0 \\ & 13.2 & 7.3 & 0 & 0 & 0 \\ & & 11.5 & 0 & 0 & 0 \\ & & & 3 & 0 & 0 \\ & & & & 2.6 & 0 \\ & & & & & 2.6 \end{bmatrix} \times 10^{-10} \frac{N}{m^2}, \quad e = \begin{bmatrix} 0 & 0 & -4.1 \\ 0 & 0 & -4.1 \\ 0 & 0 & 14.1 \\ 0 & 0 & 0 \\ 0 & 10.5 & 0 \\ 10.5 & 0 & 0 \end{bmatrix} \frac{C}{m^2}, \quad \varepsilon = \begin{bmatrix} 804.6 & 0 & 0 \\ 0 & 804.6 & 0 \\ 0 & 0 & 659.7 \end{bmatrix}$$

Material properties for the substrate layer are: elasticity modulus, $E=70\text{e}9\text{Pa}$, density, $\rho=2700\text{kg/m}^3$, Poisson' ratio, $\nu=0.3$. The dynamic move limit [7] with spatial radius $r_{\min}=0.015\text{m}$ is considered.

4.1 Actuation

4.1.1 First solution

In this example, the aim of the optimal design is to maximize the overall vertical deflection of the structure. The representative point is a point located at the middle of the free end. Structure is a two-layer plate comprises of a host layer and a PZT-4 layer with the voltage 1 volt applied in the thickness direction. For this example, the physical response function presented in equation (15) is applied.

The optimum distribution of the material is shown in Figure 2a, and the iteration curve of the objective function is shown in Figure 2b.

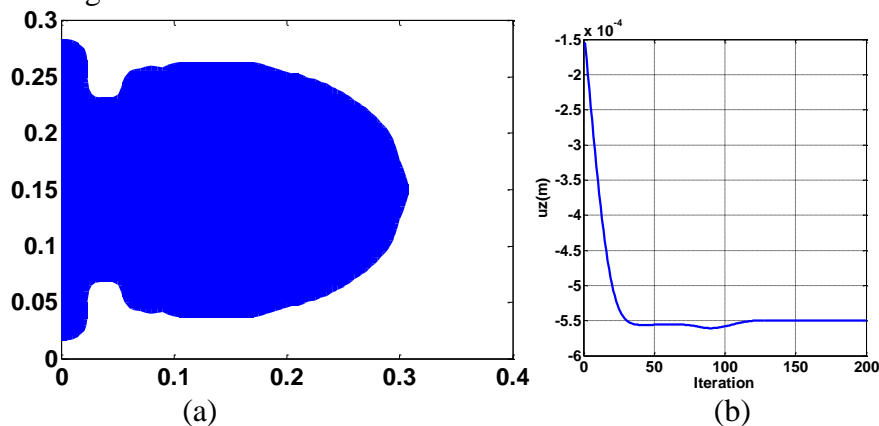


Figure 2. Optimal layout (a) and iteration histories (b) of a multilayer plate for overall displacement minimization problem.

It is observed that PZT materials are distributed mostly near the clamped edge. It is seen that the deflection of the representative point which is the point located at the middle free edge, is maximized from -0.15mm to -0.56mm.

4.1.2 Second solution

The next example is presented to demonstrate the use of the second resolution in improving the actuation effect. The idea is to maximize the deflection of the point at the middle of the free edge under the thickness direction. The FEM process was conducted two times, once with applying voltage and the next time without applying voltage and applying a unit dummy load at the proposed point and mentioned direction. By utilizing the Φ_2 physical response function, Figure 3a depicts the optimal layout of PZT layer to achieve an optimal maximized deflection.

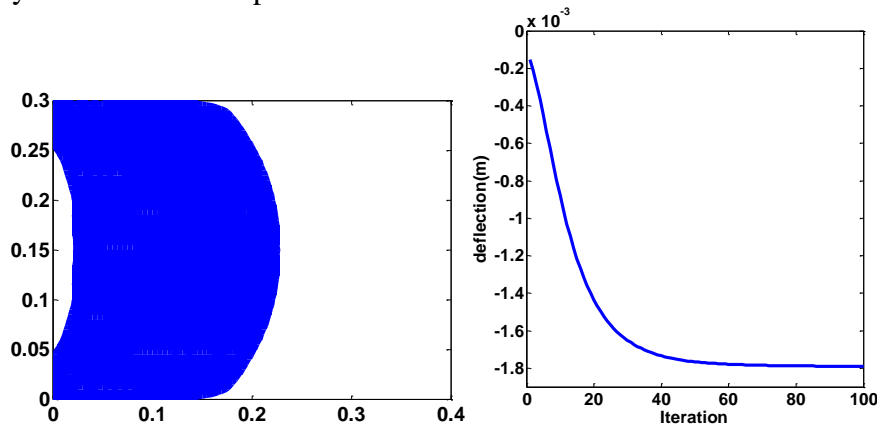


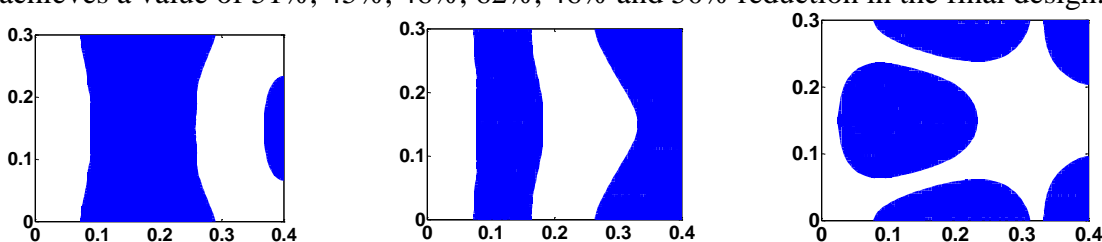
Figure 3. Optimal layout (a) and iteration histories of objective function (b) for optimization problem of reducing the deflection of an observation point.

Optimal layout features a distribution of PZT material mostly near the clamped edge in a circular shape. The evolution histories of objective function alongside of iteration number is plotted in Figure 3b. By analyzing the derived curve, it can be noticed that the objective function which is -0.15mm at the first iteration reaches to a stable final value -1.78mm which is a substantial declination.

4.2 Energy harvesting

Here we consider the design of clamped plate mentioned in previous example as shown in Figure 1a. The plate is subject to harmonic excitations of 50Hz, 100Hz, 250Hz, 500Hz, 1000Hz and 2000Hz, and magnitude of 1000N at the middle of free edge normal to the plane of the plate. The polarization direction is in the thickness direction with 1000V with the same material properties, meshing scheme, geometrical dimensions and optimization parameters as previous example. The objective of the example is to determine the optimal layout of piezoelectric material on top of a substrate such that the power dissipated is maximized or in another word the energy conversion ξ_1 is minimized. To conduct the optimization process, the physical response function Φ_3 is employed. The resulting optimal material layouts are shown in Figure 4 for each excitation frequency.

The optimal layout demonstrates a distribution of PZT materials in the form of discrete parts in the middle and right sides. In the subsequent topology optimization, the optimization process converges after 30 iterations for most of the excitation frequencies as shown in Figure 1b, from which we can see that the energy conversion factor of the piezoelectric energy harvester ξ_1 declines gradually and achieves a value of 51%, 45%, 46%, 62%, 46% and 50% reduction in the final design.



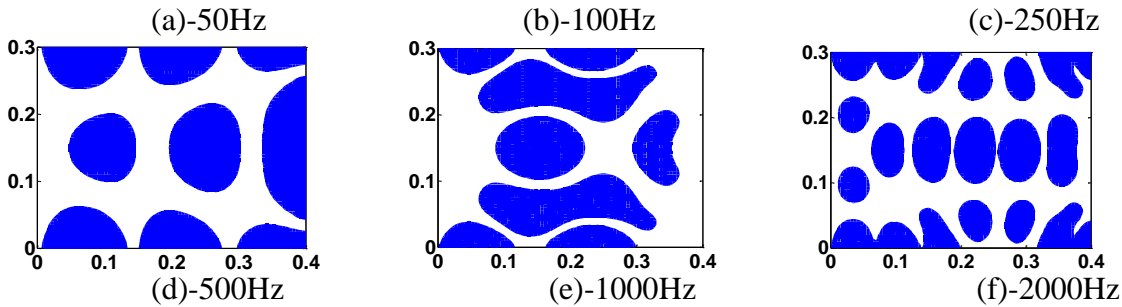


Figure 4. Optimal layout of multilayer plate under different frequencies and

5. Conclusion

The novel formulations and procedures of TO using MIST for multilayer structural plate are derived and applied to piezoelectric layers and substrates. Numerical computations determine that the proposed methodologies are effectual to minimize the overall displacement and deflection of a representative point and maximize the electromechanical coupling efficiency. Numerical results point out that the present MIST algorithm can produce optimal layouts of piezoelectric plates to address the objective functions by applying a mechanical force or electrical voltage. It is observed that in case of displacement minimization, most of the PZT materials are distributed near the clamped edges where the most strain energy are lied and a considerable declination in overall displacement or deflection of a chosen point is attained. Through the numerical example related to the energy harvesting device, it is found that about 50% in maximization of energy harvesting can be achievable for each frequency and PZT materials are covered around the middle and right sides of plate.

6. References

1. He, M., et al., *Multi-material topology optimization of piezoelectric composite structures for energy harvesting*. Composite Structures, 2021. **265**: p. 113783.
2. Kiyono, C., E. Silva, and J. Reddy, *Optimal design of laminated piezocomposite energy harvesting devices considering stress constraints*. International journal for numerical methods in engineering, 2016. **105**(12): p. 883-914.
3. Noh, J.Y. and G.H. Yoon, *Topology optimization of piezoelectric energy harvesting devices considering static and harmonic dynamic loads*. Advances in Engineering Software, 2012. **53**: p. 45-60.
4. Amlashi, A.H., A. Mohand-Ousaid, and M. Rakotondrabe. *Topology optimization of piezoelectric plate energy harvester under external in-plan force considering different boundary conditions*. in *2019 International Conference on Manipulation, Automation and Robotics at Small Scales (MARSS)*. 2019. IEEE.
5. Zheng, B., C.-J. Chang, and H.C. Gea, *Topology optimization of energy harvesting devices using piezoelectric materials*. Structural and Multidisciplinary Optimization, 2009. **38**(1): p. 17-23.
6. Kang, Z. and X. Wang, *Topology optimization of bending actuators with multilayer piezoelectric material*. Smart Materials and Structures, 2010. **19**(7): p. 075018.
7. Luo, Q. and L. Tong, *Design and testing for shape control of piezoelectric structures using topology optimization*. Engineering Structures, 2015. **97**: p. 90-104.
8. Lerch, R., *Simulation of piezoelectric devices by two-and three-dimensional finite elements*. IEEE transactions on ultrasonics, ferroelectrics, and frequency control, 1990. **37**(3): p. 233-247.